Instrumentation Science & Technology
Publication details, including instructions for authors and subscription information:
http://www.tandfonline.com/loi/list20

A Comparison of Fluorescence Inner-Filter Effects for Different Cell Configurations

Shangming Kao [a] , Alexander N. Asanov [a] & Philip B. Oldham [a]
[a] Department of Chemistry, Box 9573 Mississippi State, MS 39762

Available online: 22 Aug 2006

To cite this article: Shangming Kao, Alexander N. Asanov & Philip B. Oldham (1998): A Comparison of Fluorescence Inner-Filter Effects for Different Cell Configurations, Instrumentation Science & Technology, 26:4, 375-387

To link to this article: http://dx.doi.org/10.1080/10739149808001906

INSTRUMENTATION SCIENCE & TECHNOLOGY, 26(4), 375–387 (1998)

A COMPARISON OF FLUORESCENCE INNER-FILTER EFFECTS FOR DIFFERENT CELL CONFIGURATIONS

Shangming Kao, Alexander N. Asanov, Philip B. Oldham*

Department of Chemistry
Box 9573
Mississippi State, MS 39762

ABSTRACT

In conventional fluorescence spectroscopy, fluorescence intensity at high fluorophore concentration is often not proportional to fluorophore concentration, owing to primary and secondary absorption (inner-filter effects). In this paper, fluorescence calibration curves for anthracene solutions were obtained using a conventional right angle cell, a frontal reflection cell, a short pass cell, and a total internal reflection fluorescence (TIRF) cell for comparing the observed primary inner-filter effects. Measurements were also made of a two-component mixture using the non-fluorescent 9-nitrofluorene with anthracene for comparing primary and secondary inner-filter effects. A conventional right angle cell exhibited the widest linear dynamic range and lowest detectable anthracene concentration, whereas the TIRF cell provided the best linearity at high concentrations. The TIRF cell was determined to have significant potential for quantitative analysis of highly concentrated and/or turbid solutions.

INTRODUCTION

The popularity of fluorescence spectroscopy as an analytical tool can be attributed to its high sensitivity and selectivity. Fluorescence is appropriately used in a number of applications when a trace amount of fluorophore must be detected in a small volume sample. However, for reliable quantitative analysis of concentrated samples, problems inherent to the conventional right angle sampling geometry hinder the use of fluorescence spectroscopy. Among these, primary and secondary absorption of light are dominant. These two absorption processes are the so-called inner-filter effects (IFEs)

which typically restrict the application of fluorescence spectroscopy to dilute solutions (absorbance < 0.01). This significantly limits any potential application of fluorescence spectroscopy to industrial process monitoring and/or control.

Theoretically, the relationship between fluorescence intensity and fluorophore concentration is not linear.[1] The basic equation defining this is:

$$I_f = I_0\Phi_f(1 - e^{-\varepsilon bc}) \quad (1)$$

where I_f is the observed fluorescence intensity, I_0 is the incident light intensity, Φ_f is the fluorescence quantum efficiency, ε is the molar extinction coefficient, b is the cell pathlength, and c is the fluorophore concentration. The fluorescence intensity is, thus, logarithmically dependent on fluorophore concentration. For dilute solutions, where εbc is less than 0.01, this equation reduces to:

$$I_f = KI_0\Phi_f\varepsilon bc \quad (2)$$

with only approximately 1% errors, where K is a proportionality constant. This equation is generally used for fluorescence quantitative analysis in dilute solution.[1]

In concentrated solutions (absorbance > 0.01), fluorescence is not uniformly distributed because the excitation radiation is absorbed significantly by the fluorophore or other chromophores as it enters the cell. This is called primary inner-filter effect. The emitted fluorescence can also be absorbed by an appropriately absorbing component in the solution. This is referred to as secondary inner-filter effect. Usually, primary IFE is much more serious because excitation wavelengths are always shorter than emission wavelength, and shorter wavelengths are commonly absorbed to a greater extent in organic samples. Inner-filter effects are often responsible for distorted excitation and emission spectra and nonlinear calibration curves between fluorescence intensity and fluorophore concentration. This is particularly true at high concentrations.

A number of approaches have appeared in the literature to minimize or correct for IFE either instrumentally or by using on-line mathematical corrections. On-line corrections are based on models that lead to accurate and valid results for a wide range of chemical systems. These correction techniques include the moving mirror methods,[2,3] cell shift methods,[4-6] cell rotation methods,[7,8] calibration methods,[9] and double pass cell.[10,11] Yappert and Ingle[12-14] developed a spectrometer which allows rapid simultaneous acquisition of fluorescence and absorbance data. The measured absorbance is utilized to automatically correct the observed fluorescence for IFEs according to a mathematical model. Subbarao and MacDonald[15] gave an empirical procedure for the correction of measured fluorescence intensity for the inner-filter effect. The procedure made possible studies of protein fluorescence quenching by agents previously unsuitable because of high absorbance. Kubista et al.[16] proposed a simple and easy approach to calibrate the primary inner-filter effect from a particular experimental set-up. Konstantinov et al.[17] proposed a real-time algorithm for elimination of the inner-filter effect in a bioreactor. Recently, Victor and Crouch[18] designed a bifurcated fiber-optic-based diode array fluorometer that simultaneously measured front-surface fluorescence and absorbance.

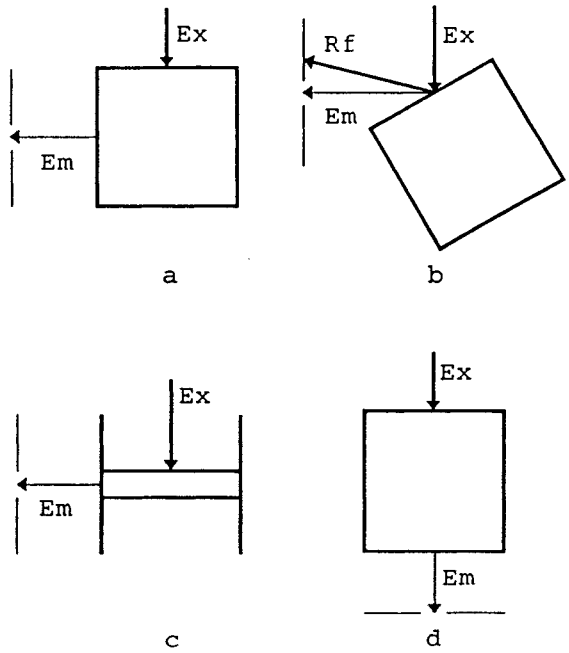

Figure 1. Top view of common cell geometries. Ex, Em, and Rf represent excitation, emission, and reflected light, respectively. a. Right angle configuration; b. Frontal geometry; c. Short-path cell; d. In-line geometry.

Instrumental corrections are based on the observation that fluorescence intensity and fluorophore concentration are linear at low absorbance. Over a period of several years, various experimental methods have been utilized to reduce IFEs. In principle, any method that can lower the absorbance will reduce IFEs. Sample dilution[1,19] is the most popular approach. However, in the case of low fluorophore concentration and high solution absorbance, due to the presence of other absorbing species, dilution will not increase determination accuracy. Additionally, dilution may cause changes in conformation, bonding, solvation, and the degree of association, as well as other chemical events which may alter absorption-fluorescence processes and, thereby, introduce large unknown errors.[3]

Different excitation and emission wavelengths can sometimes be selected where the primary or secondary absorptions are low. In these cases, the relevant molar extinction coefficients are simply exchanged. However, determination of these wavelengths are frequently difficult or even impossible.[9] Different cell configurations have also been used to reduce the optical pathlength.[1,20] Figure 1 illustrates the most common cell geometries. The right angle configuration is most common because, at this angle, the elastic scattering signal is the least intense and the contribution of cell wall fluorescence is reduced, because the walls directly illuminated by the excitation beam are not directly viewed.[21] A frontal geometry[20] is often used for solutions of high

absorbance or opacity, and for solid samples. Short pass cells[1] are designed to reduce the pathlength along a particular optical axis, usually excitation, so the primary IFE are reduced.

The pathlength of a typical right angle cell is 10 mm. For a short path cell, it may be reduced to 0.1 mm. The in-line geometry [20] is better than frontal geometry in that it is much easier to set up, and the observed intensity is much less critically dependent upon the exact position of the sample cuvet. Another advantage of the in-line arrangement is that it permits precise comparison of the intensity of fluorescence from solutions contained in cylindrical cells. But, a double monochromator is required to analyze the fluorescence emission; otherwise, the unabsorbed excitation beam enters the analyzing monochromator, directly resulting in a very high instrumental blank signal.

The capability of total internal reflection fluorescence spectroscopy to analyze strongly absorbing samples was first reported in 1965 by Hirschfeld.[22] Later, in 1987, Angel[23] reiterated the ability of TIRF to avoid inner-filter effects. However, a comparative study of IFEs using various cell designs, including TIRF, has not, until now, been undertaken. The objectives of this study are to compare the IFEs in conventional cells and to reduce the IFEs by using a total internal reflection optical scheme.

THEORY

The principles of total internal reflection are well documented in the literature.[24-26] When light propagating within a medium of refractive index (n_1) encounters a medium of lower refractive index (n_2), total internal reflection may occur if the incident angle (θ) exceeds the critical angle (θ_c):

$$\theta_c = \sin^{-1}(n_2/n_1) \tag{3}$$

Although the incident light totally reflects at the interface, a portion of the electromagnetic radiation penetrates the interface into the less dense medium. The intensity of this interfacial field, typically called the "evanescent wave," decays exponentially with distance from the interface (z):

$$E(z) = E_0\exp(-z/d_p) \tag{4}$$

where E(z) is the amplitude of the electric vector of the electromagnetic wave, as a function of the distance (z) from the interface, and E_0 is the amplitude at the interface. The penetration depth (d_p) of the evanescent wave in the less dense medium is a function of the incident angle, refractive index ratio, and incident light wavelength (λ).

$$d_p = \frac{\lambda}{2\pi\left[\sin^2\theta - \left(n_2/n_1\right)^2\right]^{1/2}} \tag{5}$$

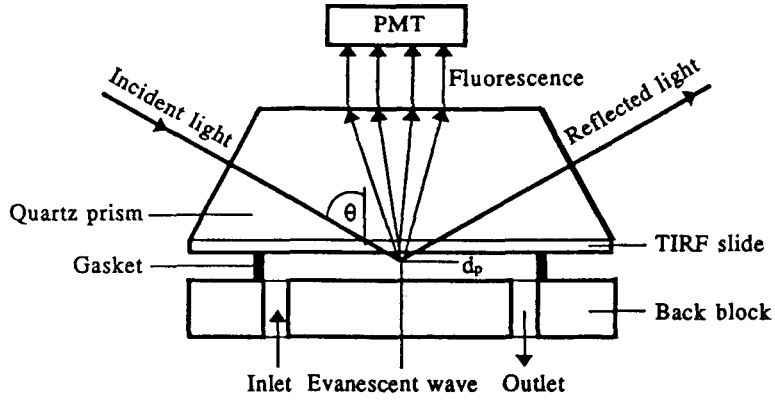

Figure 2. Schematic diagram of TIRF cell.

Evanescent wave penetration depths (d_p) are generally similar in magnitude to the wavelength of the incident light (100-400 nm in UV-Vis). The fluorophore present in the lower refractive index medium can thus be excited by the evanescent wave. The extremely short pathlength of the evanescent wave excites a very small sample volume and, thereby, minimizes primary absorption effects. Also, the emitted fluorescence detected through the waveguide does not pass through the bulk of solution, thus avoiding any secondary absorption effects. Generally, for single reflection TIRF, there is a loss of sensitivity compared to conventional optics, but some sensitivity can be recovered by utilizing multiple reflection TIRF.

EXPERIMENTAL

Spectroanalytical grade methanol, purchased from Fisher Scientific (Fair Lawn, NJ), was used as received. Anthracene (99.9%) and 9-nitrofluorene (98%) were obtained from Aldrich Chemical Company, Inc. (Milwaukee, WI). Solutions were prepared in volumetric glassware and stored in Wheaton liquid scintillation vials prior to measurements.

An Aminco-Bowman Series 2 luminescence spectrometer was used to measure the fluorescence spectra and calibration curves. Ultraviolet and visible spectral and absorbance readings were made using a HP 8452A spectrophotometer. Refractive indices were determined using a Carl Zeiss Abbe refractometer (Germany).

Normal right angle and frontal reflection geometry measurements were obtained using a conventional 10 × 10 mm square quartz florescence cell. The short path measurements used a 1 × 10 mm quartz cell. A TIRF flow cell, ISS, Inc. (Champaign, IL) was modified in our laboratory in order to obtain a chemically resistant flow system suitable for working with organic solvents.

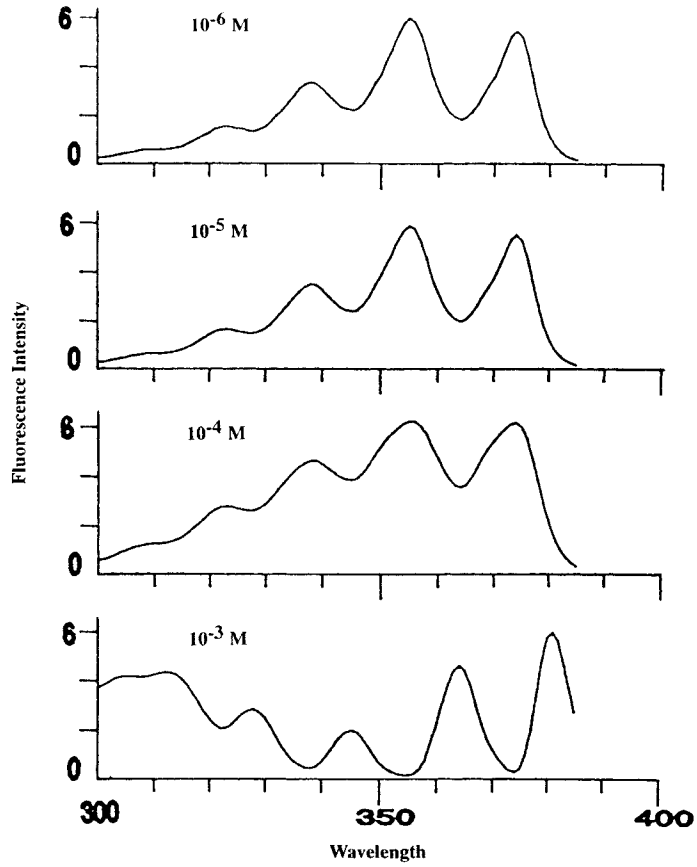

Figure 3. Excitation spectra of anthracene methanol solutions in a normal right angle cell.

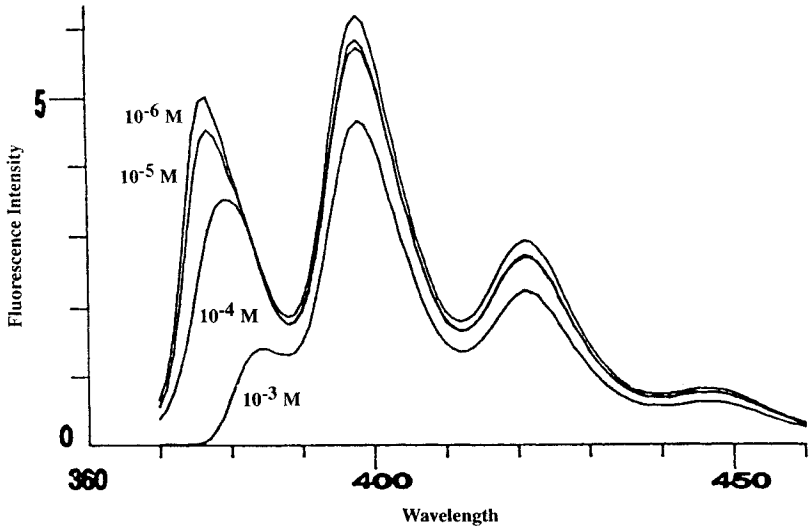

Figure 4. Emission spectra of anthracene methanol solutions in a normal right angle cell.

Figure 2 is a schematic diagram of the TIRF cell. It consists of a quartz dovetail prism, an 1 mm quartz slide (TIRF slide), a supporting back block, and a Teflon gasket. The TIRF slide is used to reduce the risk of damaging the quartz prism. An optical contact between these two parts is provided by glycerol with a refractive index close to that of quartz. The TIRF slide surface adjacent to the solution flow is the working surface in contact with the sample solution. This side of the TIRF slide may be covered by a film of any transparent material (i.e., polymeric film, C-18 layer, inorganic conducting film, etc.). In our experiments, two types of TIRF surfaces were used. A bare quartz surface was used as a model hydrophilic surface. In aqueous solution, this surface is negatively charged and demonstrates highly hydrophilic properties. Hydrophobic model surfaces were prepared by treatment of the TIRF slide with an alkylsilane (Sigmacote, Sigma Catalog No. SL-2).

An opening in the Teflon gasket forms a thin (~0.15 mm) flow chamber between the TIRF slide and the supporting back block. Two holes in the block serve to channel the solution into the flow chamber between the TIRF slide and the back block. Teflon connections and chemically resistant Hamilton valves, along with the chemically inert Teflon gasket and quartz back block, form a chemically inert flow system.

It is seen, in Figure 2, that sample within the thin layer is excited by the evanescent wave. Fluorescence is emitted in all directions with a substantial portion of it collected and detected through the prism. The TIRF cell is mounted into the sample compartment of the AB2 spectrofluorometer. The incidence angle, θ, is fixed at 73°. Therefore, an incident light wavelength of 355 nm provides a penetration depth of the evanescent wave of approximately 150 nm.

RESULTS AND DISCUSSION

Absorption effects can distort fluorescence spectral profiles. Excitation spectra of anthracene in methanol at different concentrations, obtained by using a right angle cell, are shown in Figure 3. At 10^{-6} M and 10^{-5} M, there is no primary IFE. At 10^{-4} M, IFE are indicated by comparing the intensities of the 355 nm peak and the 398 nm peak. At 10^{-6} M and 10^{-5} M, the 355 nm peak is slightly higher than the 398 nm peak. However, at 10^{-4} M, the 398 nm peak is larger. When IFE occurs, the shorter wavelength peak is generally attenuated. Serious IFE occurs at 10^{-3} M, where the excitation peaks are distorted toward longer wavelengths. Figure 4 shows the emission spectra of the same solutions. Compared to the excitation spectra, emission spectra are less subject to IFE. Only the shortest wavelength peak is attenuated, and its peak position is shifted towards longer wavelength. For frontal geometry and the short pass cell measurements, inner-filter effects occur at about 10^{-3} M and are not so obvious as those in the right angle cell. Otherwise, the trends of spectral changes are similar to those in a normal right angle cell.

Figure 5 provides the excitation and emission spectra of 10^{-3} M anthracene obtained using the TIRF cell. Very modest IFEs are indicated because the 355 nm excitation peak and the shortest wavelength emission peak are slightly attenuated. Compared to those obtained by the normal right angle cell, the adverse effects are very

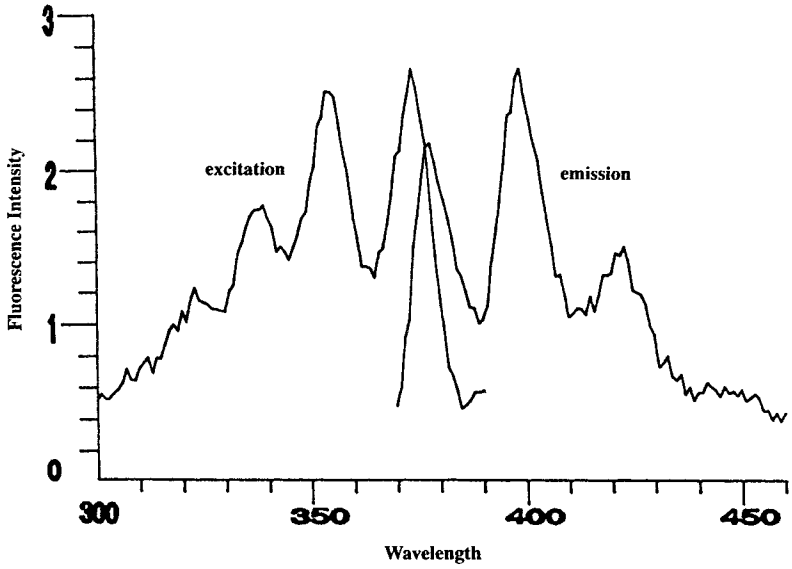

Figure 5. Excitation and emission spectra of 10^{-3} M anthracene methanol solution in a TIRF cell.

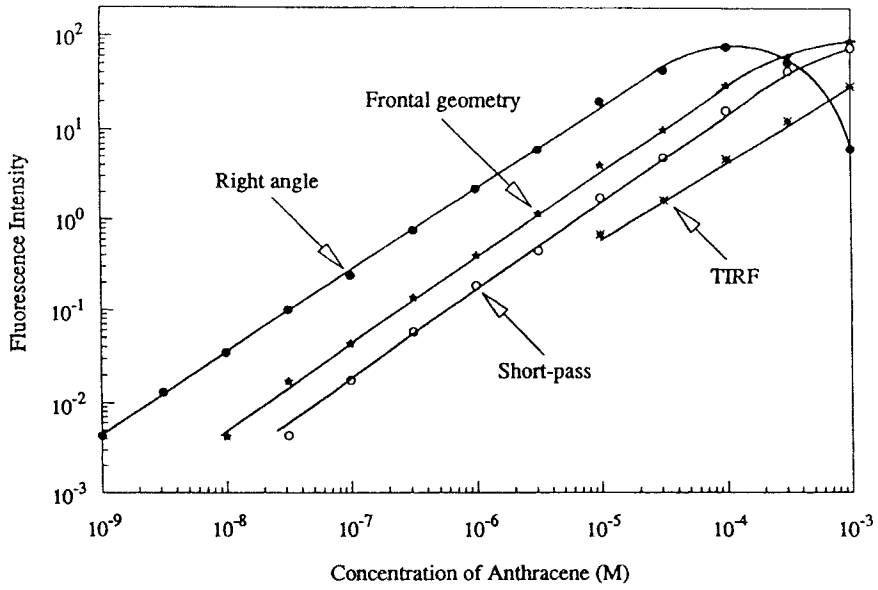

Figure 6. Calibration curves of anthracene in methanol solutions.

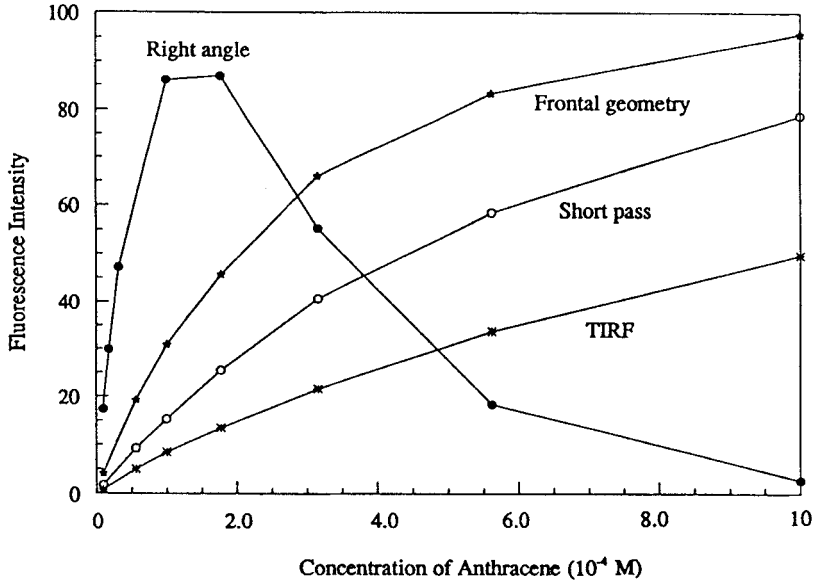

Figure 7. Calibration curves of anthracene at high concentrations in methanol solutions.

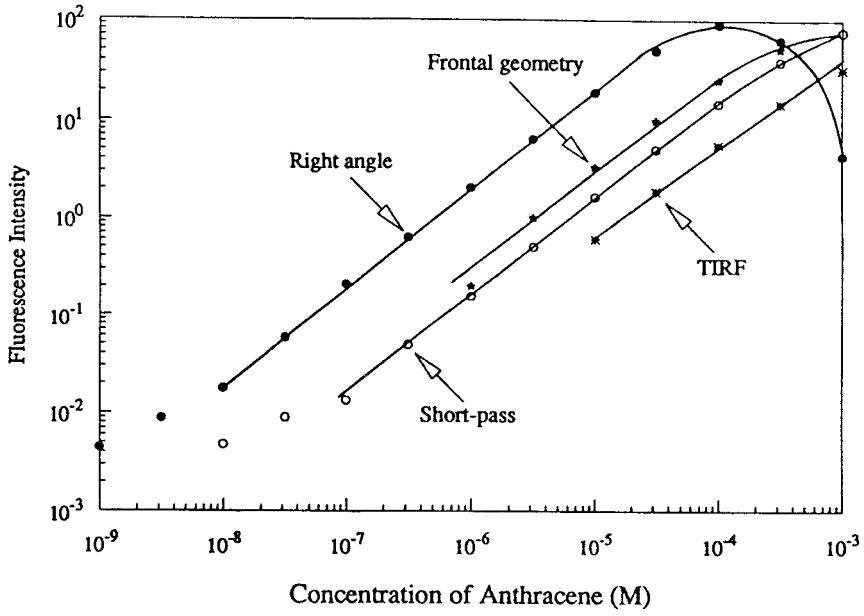

Figure 8. Calibration curves of anthracene in 10^{-5} M 9-nitrofluorene methanol solution.

weak. Figure 6 illustrates the calibration curves of anthracene in methanol, obtained by using the four different cells. The widest linear dynamic range and the lowest detectable anthracene concentrations were observed using the normal right angle geometry. However, the IFEs were reduced to various extents when using the other cells. The TIRF cell exhibited the best linearity at high sample concentrations, thus avoiding sample dilution for quantitation in this concentration range. Figure 7 shows the fluorescence intensity versus anthracene concentration at relatively high concentrations. Again, the best linear relationship was obtained by using the TIRF cell.

Figure 8 presents the calibration curves of anthracene in 10^{-5} M 9-nitrofluorene obtained by using the four different cells. 9-Nitrofluorene does not fluoresce, but it was used to model background absorbance giving rise to primary IFE. The trends are similar to those of pure anthracene in methanol. However, because of the background absorption of 9-nitrofluorene, the lowest detectable anthracene concentrations are increased.

The total absorbance of sample solutions at excitation and emission wavelengths was also measured and are listed in Table 1. 9-Nitrofluorene does not absorb at 398 nm, so it should not cause secondary inner-filter effect at this wavelength. But, it has an absorption peak at 355 nm which causes primary inner-filter effect in the determination of anthracene calibration curves.

At low anthracene concentrations, the absorbance of anthracene is smaller than that of 9-nitrofluorene, so the lowest detectable anthracene concentration is increased. At high anthracene concentrations, where the absorbance of anthracene is larger, the influence from 9-nitrofluorene is reduced.

In principle, there should be no observable IFEs in the TIRF cell within this concentration range. However, the calibration curve obtained by the TIRF cell is not perfectly linear. One possible explanation is due to the molar extinction coefficient (ε) dependence on the refractive index of the solution.

A correction[27] of this effect can be made by substituting the quantity $\varepsilon n/(n^2 + 2)^{1/2}$ for ε in equations 1 and 2. The measured refractive indexes of methanol and 10^{-3}M anthracene methanol solution are 1.3277 and 1.3282, respectively. The refractive index changes are negligible and cannot lead to the nonlinearity indicated in the calibration curve.

Since TIRF spectroscopy is an interfacial technique, the interaction between solute and surface may have a strong influence on the spectroscopic results. The first series of experiments were performed using an alkylsilane-treated quartz TIRF slide. Anthracene is a non-polar compound; it was seriously adsorbed onto this non-polar surface. The adsorbed anthracene could not be totally removed from the surface by washing with methanol. In this situation, the bare quartz slide, which has a polar surface, provided a better working surface. Although anthracene is easily removed from a hydrophilic surface, at 10^{-3} M, the anthracene solution is nearly saturated, which may lead to significant surface adsorption.

Table 1

Total Absorbance of Sample Solutions at Excitation and Emission Wavelengths

		Anthracene Conc'n (M)			
		10^{-6}	10^{-5}	10^{-4}	10^{-3}
Absorbance of Anthracene	λ_{ex} = 356 nm	0.0461	0.1218	0.8044	2.913
	λ_{em} = 398 nm	0.0348	0.0370	0.0386	0.0473
Absorbance of Anthracene in 10^{-5}M 9-Nitrofluorene	λ_{ex} = 356 nm	0.2150	0.2787	0.9486	2.936
	λ_{em} = 398 nm	0.0510	0.0431	0.0435	0.0508

Therefore, the observed effect is likely attributable to either analyte-surface interactions or some undetermined instrumental artifact. In general, one can expect that the use of a non-polar surface for polar analytes and a polar surface for non-polar analytes tends to minimize adsorptive interference.

CONCLUSIONS

Normal right angle measurements provided the widest linear dynamic range and the lowest detectable anthracene concentration, which is due to the long optical pathlength and large detection volume of this cell. However, very serious inner-filter effects were observed in the normal right angle cell. The excitation and emission spectra were distorted, even at an anthracene concentration of 10^{-4} M. Inner-filter effects were still significant, but reduced by using the frontal reflection geometry or the short path cell. However, minimal spectral distortions were observed in the TIRF measurements, providing improved detection linearity at high concentrations. Thus, TIRF appears to largely eliminate inner-filter effects.

This work has successfully demonstrated the great potential of TIRF for quantitative analysis of high fluorophore concentrations without the necessity of dilution. The TIRF optical layout discussed here may not be currently feasible in all spectrofluorometers. Therefore, it will be necessary to design a reasonably priced TIRF cell which can be mounted in conventional spectrometer sample compartments with ease and simplicity. Such a device should transform what is currently a rather esoteric sampling technique into an essentially routine analytical tool.

ACKNOWLEDGMENTS

Acknowledgement is made to Wood Utilization Research Program and NSF EPSCoR (EHR-9108767) for the financial support of this research. This paper was presented, in part, at the 1996 Pittsburgh Conference in Chicago, Illinois.

REFERENCES

1. G. G. Guilbault, **Practical Fluorescence**, Marcel Dekker, Inc., New York, 1990.
2. J. F. Holland, R. E. Teets, A. Timnick, Anal.Chem., **45**, 145-153 (1973).
3. J. F. Holland, R. E. Teets, P. M. Kelly, A. Timnick, Anal. Chem., **49**, 706-710 (1977).
4. A. Novak, Coll. Czech. Chem. Comm., **43**, 4869 (1978).
5. D. R. Christmann, S. R. Crouch, A. Timnick, Anal. Chem., **53**, 276-280 (1981).
6. D. R. Christmann, S. R. Crouch, A. Timnick, Anal. Chem., **53**, 2040-2044 (1981).
7. K. Adamsons, A. Timnick, J. F. Holland, J. E. Sell, Anal. Chem., **54**, 2186-2190 (1982).
8. K. Adamsons, J. E. Sell, J. F. Holland, A. Timnick, Amer. Lab., November, 16-29 (1984).
9. D. R. Christmann, S. R. Crouch, J. F. Holland, A. Timnick, Anal. Chem., **52**, 291-295 (1980).
10. K. W. Street, Jr., Analyst, **110**, 1169-1172 (1985).
11. K. W. Street, Jr., Analyst, **112**, 167-169 (1987).
12. M. C. Yappert, M. W. Schuyler, J. D. Ingle, Jr., Anal.Chem., **61**, 593-600 (1989).
13. M. C. Yappert, J. D. Ingle, Jr., Appl. Spectrosc., **43**, 759-767 (1989).
14. M. C. Yappert, J. D. Ingle, Jr., Appl. Spectrosc., **43**, 767-771 (1989).
15. N. K. Subbarao, R. C. MacDonald, Analyst, **118**, 913-916 (1993).
16. M. Kubista, R. Sojoback, S. Eriksson, B. Albinsson, Analyst, **119**, 417-419 (1994).
17. K. B. Konstantinov, P. Dhurjati, T. V. Dyk, W. Majarian, R. LaRossa, Biotechnology and Bioengineering., **42**, 1190-1198 (1993).
18. M. A. Victor, S. R. Crouch, Appl. Spectrosc., **49**, 1041-1047 (1995).
19. J. R. Lakowicz, **Principles of Fluorescence Spectroscopy**, Plenum Press, New York, 1986.
20. C. A. Parker, **Photoluminescence of Solutions**, Elsevier, Amsterdam, 1968.

21. J. D. Ingle, Jr., S. R. Crouch, **Spectrochemical Analysis**, Prentice-Hall, Inc. 1988.

22. T. Hirschfeld, Canad. Spectrosc., **10**, 128 (1965).

23. S. M. Angel, Spectroscopy, **2(4)**, 38 (1987).

24. N. J. Harrick, **Internal Reflection Spectroscopy**, Harrick Scientific Corp., New York, 1979.

25. E. Lee, R. E. Benner, J. B. Fenn, R. K. Chang, Appl. Opt., **18**, 862-868 (1979).

26. W. M. Reichert, P. A. Suci, J. T. Ives, J. D. Andrade, Appl. Spectrosc., **41**, 503-508 (1987).

27. D. A. Skoog, J. J. Leary, **Principles of Instrumental Analysis**, Saunders College Publishing, 1992.

Received August 29, 1997
Accepted September 23, 1997
Manuscript 1158